

UC San Diego

UC San Diego Previously Published Works

Title

Unsaturated geotechnics applied to geoenvironmental engineering problems involving geosynthetics

Permalink

<https://escholarship.org/uc/item/52s2b87d>

Authors

Bouazza, Abdelmalek
Zornberg, Jorge
McCartney, John S
[et al.](#)

Publication Date

2013-10-01

DOI

10.1016/j.enggeo.2012.11.018

Peer reviewed

1
2
3
4
5
6
7
8
9
10
11
12
13
14
15
16
17
18
19
20
21
22
23
24
25
26
27
28
29
30
31
32
33
34
35
36
37
38

Unsaturated Geotechnics Applied to Geoenvironmental Engineering Problems Involving Geosynthetics

A. Bouazza¹

Jorge Zornberg²

John S. McCartney³

Rao M. Singh⁴

¹ Professor, Monash University, Department of Civil Engineering, Bldg.60, Clayton, Melbourne, Vic. 3800, Australia. Email: malek.bouazza@monash.edu, Telephone: 61/3-9905 4956.

² Professor, The University of Texas at Austin, Civil Engineering Department-GEO, 1 University Station C1792 Austin, TX 78712-0280, USA. E-mail: zornberg@mail.utexas.edu, Telephone: 1/512-232-3595.

³ Assistant Professor and Barry Faculty Fellow, University of Colorado at Boulder, Department of Civil, Environmental, and Architectural Engineering, UCB 428, Boulder, Colorado 80309. USA. E-mail: john.mccartney@colorado.edu, Telephone: 1/303-492-0492.

⁴ Research Fellow, Monash University, Department of Civil Engineering, Bldg.60, Clayton, Melbourne, Vic. 3800, Australia. Email: rao.singh@monash.edu, Telephone: 61/3-9905 4981.

39 **Abstract**

40

41 Movement of fluids in the unsaturated zone plays an important role in many geoenvironmental
42 engineering problems. Examples include cover and basal liner systems for waste containment
43 facilities where geosynthetics are widely used and soil remediation processes, amongst many other
44 examples. This paper highlights the importance of assessing the unsaturated characteristics of
45 geosynthetics and their influence on the behaviour of engineered systems where soils and
46 geosynthetics interact under unsaturated conditions. It includes information on the water retention
47 curve and hydraulic conductivity function of geosynthetics such as geotextiles and geosynthetic
48 clay liners (GCLs) with particular focus on capillary barriers, liner performance under elevated
49 temperatures, and interface friction respectively. Effect on soil remediation is also discussed.
50 Mechanisms involved in the development of capillary barriers are evaluated to explain the storage
51 of water at the interface between materials with contrasting hydraulic conductivity (e.g. a fine-
52 grained soil and a nonwoven geotextile). Potential desiccation of GCLs is explained in the light of
53 an application in a liquid waste impoundment.

54

55

56

57

58

59

60

61

62

63

64

65

66

67

68

69 **1. INTRODUCTION**

70

71 Geosynthetics are defined as planar products manufactured from polymeric materials, which are
72 used with soil, rock or other geotechnical engineering related material as an integral part of a man-
73 made project, structure, or system (ASTM 1995). There are significant number of geosynthetic
74 types and geosynthetic applications in geotechnical and geoenvironmental engineering (Bouazza et
75 al. 2002). They can be used to fulfil most of the geosynthetics functions including containment as part
76 of the liner systems of landfills and mining containment facilities and soil remediation, these functions
77 can include:

- 78 • Separation: the material is placed between two dissimilar materials so that the integrity and
79 functioning of both materials can be maintained or improved,
- 80 • Reinforcement: the material provides tensile strength in materials or systems that lacks sufficient
81 tensile capacity,
- 82 • Filtration: the material allows flow across its plane while retaining the fine particles on its
83 upstream side,
- 84 • Drainage: the material transmits fluid within the plane of their structure,
- 85 • Hydraulic/Gas Barrier: the material is relatively impervious and its sole function is to contain
86 liquids or gasses, and
- 87 • Protection: the material provides a cushion above (or below) geomembranes in order to prevent
88 damage by punctures during placement of overlying materials.

89

90 Geosynthetics may also serve multiple functions, in this case two or more individual materials are
91 laminated, bonded or needle punched together. They are referred to as geocomposites and are used
92 in drainage of fluids or waterproofing applications amongst others applications.

93

94 In most cases, geosynthetics are placed above the groundwater table where soils are under
95 unsaturated conditions. Engineering properties of unsaturated earthen systems combining soils and
96 geosynthetics can be significantly influenced by the water storage characteristics of both the soil
97 and the geosynthetic component. Exacerbating the problem further is the hydrophobicity of
98 geosynthetics due to their manufacturing process. When embedded in soils, they can influence
99 significantly the movement of water and give rise to a redistribution of the water content profile.
100 Furthermore, it is well known that the principles of water flow through unsaturated geomaterials
101 (i.e., soils or geosynthetics) are more complex than those for water through saturated media. This is
102 partly because the most important variable that governs the rate of water flow through geomaterials
103 (i.e., the hydraulic conductivity) is not constant with varying water content. Instead, the hydraulic
104 conductivity under unsaturated conditions varies with the level of water content (or suction) within
105 the geomaterial. Consequently, relative amounts of water and air in the geomaterial highly influence
106 its hydraulic behaviour. Key to the understanding of this phenomenon is the assessment of water
107 flow and storage in porous geomaterials (e.g., soils, geosynthetics) under unsaturated conditions.

108

109 This paper includes an evaluation of the hydraulic properties of geosynthetics under unsaturated
110 conditions that are relevant to waste containment liners and soil remediation. These properties
111 include the water retention curve and the hydraulic conductivity function and will focus particularly
112 on porous geosynthetics and geocomposite materials. Specific applications are discussed to
113 illustrate new opportunities that may result from a better understanding of the unsaturated hydraulic
114 properties of geosynthetics. Finally, linkages between the unsaturated hydraulic properties of
115 geosynthetics and soils and their mechanical interface behaviour are discussed.

116

117

118 2. HYDRAULIC PROPERTIES OF UNSATURATED GEOTEXTILES

119
120

121 Among the various types of geosynthetics, geotextiles have been used in geotechnical and
122 geoenvironmental engineering applications to fulfil the widest range of functions (Bouazza et al.,
123 2002, Koerner 2005, Zornberg and Christopher 2007). This includes separation between different
124 soil layers and filtration and drainage from surrounding soil amongst many other functions.
125 Geotextiles are able to meet these requirements despite their small thickness (e.g., 2.5 mm) partly
126 due to their high porosity (typically about 0.9), which is greater than that of most soils. Geotextiles
127 have a uniform pore size compared to most soils (Palmeira and Gardoni 2002, Aydilek *et al.* 2007).
128 There are two types of geotextiles: woven geotextiles and nonwoven geotextiles. Woven geotextiles
129 are manufactured using traditional weaving methods and are extensively used for reinforcement
130 purposes. Nonwoven geotextiles are manufactured by needle punching or melt bonding and are
131 extensively used for drainage, filtration, protection, and separation.

132

133 The water storage of soil and geosynthetics is typically quantified using the relationship between
134 volumetric water content and suction, referred to as the Water Retention Curve (WRC). Figure 1
135 shows the WRCs for different geotechnical materials. The coarser materials (sand and geotextile)
136 show a highly nonlinear response, with a significant decrease in water content (or degree of
137 saturation) within a comparatively narrow range of suction. The fine-grained soil shows instead a
138 more gradual decrease in water content with increasing suction. The nonlinearity observed in these
139 relationships is partly caused by the range of pore size distributions in these materials.

140

141 The WRC for a given material is not only sensitive to the pore size distribution, but also to the soil
142 mineralogy (for the case of soils), polymeric material (for the case of geosynthetics), density, and
143 pore structure (Hillel 1988, Bouazza *et al.* 2006a, 2006b). The WRC can show significantly
144 different wetting and drying paths, a phenomenon referred to as hysteresis (Topp and Miller 1966,

145 Kool and Parker 1987, Bouazza *et al.* 2006a). During drying, the largest pores drain first, followed
146 by the smaller pores. During wetting, the smaller pores fill first, but the presence of large pores
147 may prevent some of the small pores from filling. Also, wetting of a dry geomaterial often leads to
148 entrapment of air in the larger pores, preventing saturation of the media unless positive pressure is
149 applied to the water. Air entrapment causes the wetting path to be relatively flat for high suction,
150 with a steep increase in volumetric water content at lower suctions. Figure 2 shows the WRC of
151 three geotextiles illustrating the significant hysteresis in their response to wetting and drying
152 (Bouazza *et al.* 2006b). Recent experimental results highlighted also the impact on hysteresis of the
153 direction of flow measurement (Nahlawi 2009). In particular, it was found that the volumetric water
154 content of geotextiles along the cross-plane direction differed from that obtained along the in-plane
155 direction for the same suction head. Several techniques have been developed to determine
156 experimentally the WRC of soils (Wang and Benson 2004, Klute *et al.* 1986). These techniques
157 have been recently adapted to obtain experimentally the WRC of geotextiles. Two main groups of
158 techniques that have been used to define the WRC include physical techniques and thermodynamic
159 techniques; these have been summarized in details in Zornberg *et al.* (2010). The reader is referred
160 to this reference for further information.

161

162 The WRC of geomaterials is typically quantified by fitting experimental data to power law,
163 hyperbolic, or polynomial functions (Brooks and Corey 1964, van Genuchten 1980, Fredlund and
164 Xing 1994). Although the Brooks and Corey (1964) model is able to represent a sharp air entry
165 suction, the van Genuchten (1980) model has been most commonly used in numerical analyses
166 because it is differentiable for the full suction range. The van Genuchten (1980) model is given by:

167

$$\theta = \theta_r + (\theta_s - \theta_r) \left[1 + (\alpha \psi)^N \right]^{-\left(1 - \frac{1}{N}\right)} \quad [1]$$

168

169 where θ_r is the residual water content, θ_s is the saturated water content (porosity), and α (units of
170 kPa^{-1}) and N (dimensionless) are fitting parameters. Preliminary estimates of the WRC have been
171 obtained using databases that rely on the granulometric distribution of soils (Fredlund and Xing
172 1994). The functions used to fit experimental data from WRC have also been proven to be useful
173 for the case of geotextiles (Bouazza *et al.* 2006b, Nahlawi *et al.* 2007).

174

175 The relationship between hydraulic conductivity and suction, also referred to as the K -function,
176 provides a measure of the increased impedance to water flow with decreasing water content.
177 Conventional methods used to define the K -function may be costly, time consuming, and prone to
178 error due to experimental issues involved in the control of water flow through unsaturated
179 geomaterials. Accordingly, K -functions (*e.g.* such as those in Figure 3) are often predicted based on
180 the information obtained using theoretical derivations based on the measured WRC. Specifically,
181 the K -function obtained using the parameters from the van Genuchten-Mualem model (van
182 Genuchten 1980). Other predictive relationships for the K -function are given by Burdine (1953),
183 Brooks and Corey (1964) and Fredlund and Xing (1994) among others. Nahlawi *et al.* (2007a)
184 noted that the K -functions for geotextiles were better estimated by the van Genuchten WRC
185 equation because it is continuous. It is interesting to note from Figure 2 that the predictive hydraulic
186 conductivity functions indicate that the three geotextiles require suctions between 0.8 kPa and 1.2
187 kPa to induce a rapid drop in hydraulic conductivity. This indicates that the geotextiles will be able
188 to drain/filter water at very low suctions (*i.e.*, less than 1.2 kPa), whereas an increase in suction will
189 result very rapidly in a much lower water drainage/ filter capacity. The partially saturated
190 condition of geotextiles under relatively low suction has important implications to the hydraulic
191 performance of geotextiles. A consequence of low hydraulic conductivity of the geotextile is the
192 creation of a capillary barrier which can be beneficial if it was designed with this intention in mind.
193 However, if the inclusions of geotextiles reduce the ability for moisture to migrate as planned; then
194 they may not be accomplishing their intended purpose and, could even worsen rather than improve

195 the earth system performance. Iryo and Rowe (2005) noted that the formation of geosynthetic
196 capillary barrier may lead to unexpected behavior in the leak-detection or secondary leachate
197 collection system below a landfill composite liner. They concluded that the time at which leakage
198 occurs from primary landfill liner systems may be seriously overestimated.

199

200 **3. GEOTEXTILES AND UNSATURATED SOILS**

201 Many design applications involving earth structures have geotextiles placed in contact with
202 unsaturated soils, in some cases for much of their design life. In this respect, quantification of the
203 hydraulic performance of the geotextiles and their interaction with the surrounding soils is crucial to
204 the serviceability and maintenance these structures. Equally important is the assessment of the
205 unsaturated hydraulic characteristics of the soils in direct contact with the geotextiles. Considering
206 the differences in both materials, it should be expected that their unsaturated hydraulic properties to
207 affect the overall hydraulic performance of earthen systems because of the possible redistribution of
208 the water content profile.

209 Two soils were used in the testing program reported by McCartney et al. (2005), Bouazza et al.
210 (2006b) and Zornberg et al. (2010). A low plasticity clay was used as a relatively low hydraulic
211 conductivity material ($k_s = 1.23 \times 10^{-6}$ m/s). For all tests, the clay was statically compacted to a
212 relative compaction of 75% in relation to the maximum dry density of 1902 kg/m³. A coarse sand
213 was used for comparison with geosynthetic drainage layers as it has a high hydraulic conductivity
214 material ($k_s = 5.3 \times 10^{-4}$ m/s), representative of conventional drainage layers. In all tests, the sand
215 was placed at a void ratio corresponding to a relative density of 50% ($e_{max} = 0.78$, $e_{min} = 0.56$).
216 Coarse gravel with high hydraulic conductivity ($k_s = 1.3 \times 10^{-4}$ m/s) was used as a foundation layer.
217 The geocomposite drainage layer used in this study consists of a geonet sandwiched between two
218 nonwoven geotextiles ($k_{sGT} = 1.93 \times 10^{-3}$ m/s). The grain size distribution for the clay and sand are
219 shown in Figure 4, along with the apparent opening size (AOS) of the nonwoven geotextile
220 component (GT3) of the geocomposite material. This figure indicates that the clay material has a

221 wide range of particle sizes and should retain significant volume of water even when unsaturated.
222 The sand is poorly graded, with a large fraction of coarse particles, suggesting that it will drain
223 rapidly. According to Carroll's criterion ($AOS < 2.5d_{85}$), the geotextile is an acceptable filter for
224 both the silt and the sand (Koerner, 2005

225

226 Although the study involved infiltration into dry soil following the wetting-path of the soil water
227 retention curve, the drying-path defined in their work can still be used to highlight important
228 hydraulic differences between the materials. Figure 5 shows the water retention data of the three
229 materials along with the best-fit water retention curves defined using the SWRC model proposed by
230 van Genuchten (1980). The hydraulic conductivity functions shown in Figure 6 were defined using
231 the water retention curve parameters and the saturated hydraulic conductivity (k_s) values obtained
232 from flexible wall permeameter tests for both the clay and the sand. The geotextile saturated
233 hydraulic conductivity was based on the permittivity measurement as supplied by the geocomposite
234 manufacturer. The results in Figure 6 indicate that as suction increases, the hydraulic conductivity
235 values of the three materials decrease at different rates.

236

237 The k -functions in Figure 6 indicate that a capillary break is likely at the interface between the clay
238 and the nonwoven geotextile, as well as between the sand and the clay. While suction at an
239 interface between two materials is the same, Figure 6 highlights that the three tested materials may
240 have different hydraulic conductivities for a given value of suction, except when their curves
241 intersect. Specifically, in vertical, downward flow through an initially dry (high suction)
242 horizontally layered system, a capillary break will occur when the underlying layer has significantly
243 lower hydraulic conductivity than the overlying layer. Water will not flow into the lower layer until
244 the suction decreases to the value at which the conductivity of both layers is the same. This is the
245 case for the interface between the clay and the sand or between the clay and the geotextile
246 component of the geosynthetic drainage layer. Figure 5 indicates that as suction increases from 1

247 to 10 kPa, the geotextile and sand become highly unsaturated while the clay maintains a high degree
248 of saturation. Likewise, Figure 6 indicates that the hydraulic conductivity values of the geotextile
249 and sand decrease sharply with increasing suction, while that of the silt decreases more gently,
250 intersecting the other two curves at suctions of about 1 and 4.5 kPa, respectively.

251

252 **3.1 Practical implication: Capillary break phenomenon**

253

254 Geosynthetic drainage layers are commonly used in geotechnical engineering applications as a
255 drainage material for saturated soils. They typically consist of a combination of geosynthetics with
256 the objectives of providing the functions of filtration, in-plane drainage, and a separation or
257 protection layer. They are being increasingly used as alternatives to conventional sand or gravel
258 drains in landfills, roadway subgrades, mechanically stabilized walls, and dams. The geosynthetic
259 drainage layer configuration consists of a geonet for drainage sandwiched between nonwoven
260 geotextile filters. The in-plane flow through geotextiles and geonets can be reasonably defined if the
261 soil overlying the geosynthetic drainage layer is saturated. However, the overlying soil is often
262 under unsaturated conditions and, in this case, a capillary break may develop within the soil layer,
263 as discussed in the previous section. Understanding of this mechanism is relevant in aspects such as
264 quantification of the impinging flow used in the design of drainage layers, performance evaluation
265 of systems used for quantifying percolation through alternative landfill covers, and interpretation of
266 the information gathered in leak detection systems. Consequently, nonwoven geotextiles and
267 drainage geocomposites were evaluated experimentally using infiltration tests involving
268 geosynthetic-soil columns and compared to infiltrations tests in clay-sand columns (McCartney et
269 al. 2005).

270

271 A capillary break is evidenced as a cease in movement of the wetting front (the depth to which
272 water has infiltrated), and storage in the overlying material of moisture in excess of the amount that

273 would be stored when draining under gravity. When a critical suction is reached, the conductivity
274 of the two materials reaches the same value, and water breaks through the interface. This critical
275 suction is referred to as the breakthrough suction. In order to quantify the unsaturated interaction
276 between conventional and geosynthetic drainage layers with low hydraulic conductivity soils,
277 geosynthetic-soil profiles were constructed using different soil and geosynthetic materials
278 horizontally layered in cylindrical tubes with a relatively large diameter (20 cm). Figure 7 shows a
279 schematic view of two profiles that have been tested as part of the work reported by McCartney et
280 al. (2005) and Zornberg et al. (2010).

281 Column 1 includes a conventional drainage layer, consisting of clay placed over a sand layer. A
282 150 mm layer of sand was pluviated to reach the target relative density of 50%. A 300 mm layer of
283 clay was placed in 50 mm lifts over the sand layer using static compaction to the target dry unit
284 weight of 75% of the maximum dry unit weight based on the standard proctor and a gravimetric
285 moisture content of 8% (volumetric moisture content of 12%). Profile 2 includes a geosynthetic
286 drainage layer involving clay placed over a geocomposite, which in turn rests on a gravel
287 foundation layer. A 300 mm clay layer was placed in 50 mm lifts using the same procedures as for
288 Profile 1. Volumetric moisture content values were continuously measured throughout the vertical
289 soil profiles using time domain reflectometry technology (TDR). Figure 7 shows the location of the
290 TDR probes in both columns. In Column 1, four TDR probes were used. Probes were placed 2 cm
291 above and below the interface between the clay and the sand to measure the behaviour at the
292 interface. In Column 2, three probes were used; including a probe located 2 cm above the
293 geocomposite. A peristaltic pump was used to apply a relatively constant flow rate of $0.4 \text{ cm}^3/\text{s}$ to
294 the top surface of the clay. This corresponds to a Darcian velocity of $2.06 \times 10^{-7} \text{ m/s}$. The flow rate
295 was selected to be less than the saturated hydraulic conductivity of the clay to ensure unsaturated
296 conditions.

297 Figure 8 shows the change in water content at four depths in profile 1 (Column 1). This figure
298 indicates that the sand is initially very dry, at a volumetric moisture content of approximately 5%.

299 At this moisture content, the sand has low hydraulic conductivity. The clay soil is initially at a
300 volumetric moisture content of approximately 12% throughout the entire thickness of the profile.
301 The volumetric moisture content measured by TDR 1 (near the soil surface) increases to
302 approximately 25% as the moisture front advances through the clay. Similarly, the volumetric
303 moisture content measured by TDR 2 increases to 25% after a period of about 5000 minutes. The
304 volumetric moisture content measured by TDR 3 increases to 25%, similar to TDRs 1 and 2.
305 However, TDR 3 shows a continued increase in moisture content to approximately 38%. Also, after
306 approximately 7000 minutes TDR 2 begins to show an increase in a similar fashion as TDR 3. This
307 behaviour suggests that the wetting front reached the sand interface, but moisture accumulated
308 above the interface instead of flowing directly into the sand layer. After the clay reached a
309 volumetric moisture content of 38% at the interface, the volumetric moisture content in the sand
310 layer measured by TDR 4 increased rapidly to 26%. The timing of the increase in volumetric
311 moisture content in the sand layer was consistent with the collection of outflow at the base of the
312 profile, which occurred after approximately 9000 min. The performance of profile 1 is consistent
313 with the development of a capillary break, and indicates that the clay layer has a volumetric
314 moisture content of approximately 36% at breakthrough. The clay water retention curve shown in
315 Figure 5 indicates that this volumetric water content corresponds to a suction of approximately 5
316 kPa. This suction is consistent with the breakthrough suction value at which the k -functions of the
317 clay and sand intersect, as shown in Figure 6.

318 Figure 9 shows the change in volumetric water content at three depths in the clay in profile 2
319 (Column 2). Although similar behaviour as profile 1 is noted, the wetting front progresses faster
320 through profile 2. This is because of a clog that was noted in the water supply tube to Profile 1 after
321 the first 300 minutes of testing. However, comparison between the two profiles is still possible.
322 The volumetric moisture content in the clay in profile 2 is 12% at the beginning of testing. The
323 volumetric moisture content recorded by TDR 5 (near the soil surface) increases to approximately
324 25% after 2000 minutes. After approximately 3500 minutes, the volumetric moisture content

325 measured by TDR 6 also increases to approximately 25%. Unlike the other two TDRs, the
326 volumetric moisture content measured by TDR 7 (near the geocomposite) shows a continued
327 increase in moisture content to approximately 40%. After TDR 7 shows an increase in volumetric
328 moisture content, the volumetric moisture content recorded by TDRs 5 and 6 also increase from 25
329 to 40%. This behaviour suggests that a capillary break and storage of water over the geosynthetic
330 interface also occurs in profile 2. Outflow from profile 2 was detected after 8180 min, indicating
331 that the breakthrough of the capillary break occurred at a volumetric moisture content of
332 approximately 40%. The clay water retention curve shown in Figure 5 indicates that this
333 corresponds to a suction of about 3 kPa. This suction value is consistent with the intersection of the
334 *k*-functions for the clay and the geotextile given in Figure 6.

335 The results in Figures 8 and 9 indicate that similar behaviour can be expected from both
336 conventional granular drains and geosynthetic drainage layers overlain by unsaturated soil. The
337 moisture front advance was indicated by an increase in volumetric moisture content within the
338 profile to approximately 25% (the moisture content associated with the impinging flow rate).
339 However, as the wetting front reached the interfaces, the unsaturated drainage material created a
340 barrier to flow, and water accumulated above the interfaces as indicated by an increase in
341 volumetric moisture content to values ranging from 35 to 40%. Further, the soil above the interface
342 began to store water to a height of at least 250 mm, indicated by an increase in volumetric moisture
343 content measured by upper TDRs from 25% to approximately 35 to 40%. Although suction was
344 not monitored, the shape of the water retention curve for the clay indicates that the suction can
345 change significantly with small changes in moisture content near saturation. Accordingly, even
346 though moisture remained relatively constant above the interface about 1000 minutes before
347 breakthrough in both profiles, the suction was likely decreasing.

348

349 The above findings were implemented in the design and construction of alternative covers for
350 the Rocky Mountain Arsenal, a Superfund site located near Denver, Colorado (USA). In particular,

351 nonwoven geotextiles were utilized as capillary barrier material underlying a fine grained
352 unsaturated soil layer (see Zornberg et al. 2010, Williams et al. 2010, 2011).

353

354 **4. UNSATURATED BEHAVIOUR OF GEOSYNTHETIC CLAY LINERS**

355

356 Waste containment facilities form part of critical infrastructure that provides essential community
357 services. In many global population centres this vital infrastructure is designed to ensure negligible
358 long-term environmental and human health impact. To achieve these aims, construction is required
359 of barrier systems which effectively separate the waste and the associated leachate and biogas from
360 the groundwater system and the atmosphere, respectively. One conventional approach to barrier
361 systems has been to construct a “resistive barrier” composed of a capping liner that reduces water
362 ingress into the facility and controls biogas escape into the atmosphere, as well as base liner having
363 a low saturated hydraulic conductivity which minimises leachate migration out of the facility. Over
364 the past two decades, geosynthetic clay liners (GCLs) have become one of the dominant
365 construction materials in waste containment facilities and have gained widespread acceptance for
366 use in liner systems, (Bouazza 2002, Rowe 2005, Bouazza and Bowders 2010). GCLs are typically
367 comprised of a thin layer of bentonite sandwiched between two layers of geotextile with the
368 components being held together by needle-punching or stitch bonding (Figure 10). The primary
369 function of the bentonite layer in a GCL is to create impedance to the flow of migrating liquids
370 (e.g., water), dissolved chemical species and gases or vapours (Gates et al. 2009). This is achieved
371 by its very low permeability when it is fully hydrated after the GCL placement, from the underlying
372 or overlying soil.

373 However, these GCLs may be subjected to variable hydration states both during initial hydration
374 (since they are typically constructed at a low moisture content and need to be hydrated to moisture
375 content in excess of 100% to function adequately as a barrier to fluids), during thermal cycles, such
376 as may occur during wet-dry cycles or if exposed to solar radiation, and elevated temperatures at the

377 base liner which can be caused by the degradation of municipal solid waste (Rowe and Hoor 2009,
378 Bouazza et al. 2011) or mining liquors (Hornsey et al. 2010) . Hence, understanding of their water
379 potential is essential to ensure their long term durability under adverse conditions. As a fundamental
380 constitutive relationship, a water retention curve (WRC) can be used to examine their unsaturated
381 behaviour.

382 A limited number of studies have been carried out over the last decade, on water retention
383 behaviour of GCLs using different suction measurement techniques. As the key component of GCL,
384 the bentonite represents the strongest influence on the WRC. Generally, one suction measurement
385 method cannot cover the entire WRC curve, due to limits in the accuracy of each method. Different
386 direct and indirect suction measurement techniques have been used alone or in various
387 combinations to gain GCL WRC in previous studies. Daniel et al. (1993) used a vapour equilibrium
388 technique (VET). Barroso et al. (2006) used a filter paper method and obtained reasonable
389 agreement with the results of Daniel at al. (1993). Southen and Rowe (2007) used a pressure plate
390 and pressure membrane extractors to assess the relationship between the degree of saturation and
391 suction in GCLs for a range of suctions between 10 and 10,000 kPa. They also examined the effect
392 of overburden pressure together with the relationship between suction and bulk GCL void ratio.

393

394 Beddoe et al. (2010) combined high capacity tensiometer (HCT) with capacitive relative humidity
395 sensor measurements to measure the WRC of a GCL. They used a 500 kPa high air entry value
396 (HAEV) porous stone HCT to measure low suction range (up to 500 kPa) and used the capacitive
397 relative humidity sensor for the range of 10,000 kPa to 350,000 kPa. Their results could not cover
398 the range between 500 kPa to 10,000 kPa.

399

400 The complexity of GCL, with its geotextile-bentonite-geotextile sandwich pattern, in comparison
401 with a uniform material makes measurement and interpretation of WRC complex. Therefore, the
402 point of measurement, quality of measurement and device-sample contact were investigated in

403 previous studies from the perspective of obtaining the WRC of the whole material rather than just
404 the geosynthetic or the bentonite component. Barroso et al. (2006) investigated the effect of filter
405 paper position in relation to the GCL using the filter paper test. They concluded that the filter paper
406 position does not influence GCL suction measurement between gravimetric water contents of 10%
407 and 115%. Unlike Barroso et al. (2006), the study by Southen and Rowe (2007) which used an axis
408 translation technique, had considerably large scatter because of loose contact between GCL sample
409 and porous filter. Beddoe et al. (2010) installed HCT into the bentonite part of a GLC to avoid
410 contact problems during measurement. Abuel-Naga and Bouazza (2010) recommended a new
411 modified triaxial apparatus which allowed control of the wetting path water content using an
412 attached needle system in the conventional cap. They adopted a silica gel desiccator cell system
413 presented by Lourenco et al. (2007) for drying path measurements. The new triaxial system
414 combined dual suction measurement techniques of thermocouple psychrometer and a relative
415 humidity sensor.

416

417 Figure 11 presents a compilation of the volumetric water content against suction for different
418 type of GCLs on the wetting path from Abuel Naga and Bouazza (2010) and Beddoe et al. (2011).
419 GCL 2 specimen tested by Beddoe et al. (2011) is a thermally treated needle punched GCL with a
420 scrim reinforced nonwoven geotextile as the carrier (material beneath the bentonite) and a
421 nonwoven cover geotextile. It is similar to the GCL specimen tested by Abuel Naga and Bouazza
422 (2010). GCL 1 is a similar product but with a woven geotextile as a carrier.

423

424 The measurements in Figure 11 indicate that the similar GCLs have lower water uptake capacity
425 compared to GCL1. The lower water uptake capacity can be attributed to their internal structure
426 (thermally treated and scrim reinforced) thus restricting their swelling potential. The slight
427 difference in water uptake observed at higher suctions levels ($>10,000$ kPa) between the two similar
428 GCLs can be attributed to the confining stresses applied during the water retention tests (2 kPa for

429 GCL 2 and 50 kPa for the GCL specimen tested by Abuel Naga and Bouazza (2010)). It is expected
430 that a higher confining stress will restrict the GCL swelling potential further leading potentially to
431 different water retention behaviour at lower suctions. Based on the above, one can conclude that
432 the method of manufacture governs the unsaturated behaviour of GCLs. However, further work is
433 needed to investigate the effect of the bentonite components of GCLs especially in terms of
434 mineralogy and grain size.

435 From a practical view point, understanding the unsaturated behaviour of GCLs and the factors that
436 control it will lead to much better prediction of their response when subjected to conditions
437 involving thermal cycles, solar heating and wet-dry cycles typically encountered in waste
438 containment facilities.

439 **4.1 Practical Implications: Potential Desiccation of GCLs**

440

441 Landfill monitoring has shown that the heat generated by municipal solid waste, can significantly
442 increase the temperature on the underlying landfill liner. Recent data indicate that landfill liner
443 temperature can be expected to reach 30-45 °C under normal landfill operations (Yesiller et al.
444 2005; Rowe 2005; Koerner and Koerner 2006). With recirculation of leachate, the liner
445 temperature tends to increase faster than under normal operating conditions (Koerner and Koerner
446 2006). Higher temperatures (up to 70°C) may also occur at the base of landfills if there is a
447 significant leachate mound (Yoshida et al. 1996). However, high temperatures (55 to 60 °C) were
448 also observed in landfills without leachate mounding (Lefebvre et al. 2000) or in landfills where
449 organic waste was predominant (Bouazza, et al. 2011). Elevated temperatures are also present in
450 lined mining facilities (e.g., heap leach pads, liquors ponds, etc.) due to the processes involved in
451 extracting the different metals (Hornsey et al., 2010, Bouazza, 2010). Often the base barrier systems
452 involve a composite barrier comprised of a geomembrane and either a compacted clay liner or a
453 geosynthetic clay liner (GCL) with a low hydraulic conductivity. One potential consequence of the
454 presence of elevated temperatures is the development of thermal gradients across the liner towards

455 the cooler subgrade soil. A schematic of the conditions existing at the base of a containment facility
456 where for example a GCL is used in combination with a geomembrane is shown in Figure 12. The
457 presence of a thermal gradient can create a risk of outward moisture movement and possible
458 desiccation of the GCL. The situation is exacerbated by the presence of an overlying geomembrane
459 preventing rehydration of the GCL with moisture from above.

460 Vapour migration through geomaterials is an important thermo-hydraulic coupling and critical to
461 understanding the thermo-hydraulic behaviour of the majority of geoenvironmental engineering
462 problems when temperature gradients are apparent such as in the case shown in Figure 12. This
463 aspect has been recently assessed for an evaporation pond lined with a composite liner similar to the
464 one shown in Figure 12. The pond is filled with saline water, at temperature up to 70°C, generated
465 from coal seam gas production. It is lined with a composite liner consisting of a geomembrane and a
466 geosynthetic clay liner resting on a fine grained subgrade. The GCL was installed at moisture
467 content as received (i.e., GCL relatively dry) and the subgrade was compacted at optimum moisture
468 content +2%. The groundwater is relatively deep. The scenario modelled assumed the filling of the
469 pond to take place as soon as its construction was completed. The case (Figure 13) was analysed
470 using a transient finite element code COMPASS (Code for Modelling Partially Saturated Soil)
471 developed at the University of Cardiff, U.K. The governing equations for COMPASS are
472 formulated from the primary variables, pore-water pressure, u_1 , temperature, T , pore-air pressure, u_a ,
473 displacement, u , to describe the thermo-hydro- mechanical behaviour. In general terms the flow
474 variables are formed into governing equations by consideration of the conservation of mass/energy
475 and the mechanical formulation is formed by consideration of stress equilibrium, with more details
476 of the THM model found in Thomas and He (1994) and Singh (2007). Pseudo 1D axisymmetric
477 numerical analyses have been performed to investigate the heat transfer and moisture movement
478 across the profile, shown in Figure 13, representing field conditions encountered at the site of the
479 pond. A zero heat flux boundary condition was applied to the side of the domain. The water
480 retention properties of the different materials were assessed in the laboratory.

481

482 Figure 14 presents the variation of the degree of saturation across the liner and the subsoil. It can be
483 observed that the degree of saturation in the GCL (lower part at 0.0095 m) increases rapidly at the
484 beginning due to its higher suction compared to the subgrade suction. However, it peaked at around
485 55% (reached within 27 days) indicating that the GCL reached only a partially hydrated state. The
486 upper and the central parts of the GCL reached even lower degrees of saturation. Obviously with
487 heat being present from the start of the filling process and rapidly reaching steady state, hydration
488 of the whole GCL is not optimised since it is subjected to high temperatures from the start of the
489 hydration process (Figure 15). A softening of the saturation, after the peak value was reached, is
490 observed with a steady decrease occurring due to moisture being driven away by heat. The degree
491 of saturation in the subgrade decreased from the beginning to the end of the simulation (10 years
492 representing the design life of the pond). Initially moisture has been absorbed by the GCL to assist
493 in its hydration then this was followed by the effect of the heat acting on the liner reaching steady
494 state very quickly as indicated in Figure 15. The top layers of the vadose zone (within 5 m)
495 experienced an increase in the degree of saturation due to moisture migrating from the GCL and the
496 subgrade up to the stage where temperature started increase steeply, with temperatures reaching
497 steady state moisture losses started to take place leading to a softening of the saturation variation.
498 Bottom layers of the vadose zone have continuous increase of moisture with time because they are
499 being fed with the water from the top layers.

500 The modelling indicates very clearly that the operation of the pond needs to be carefully planned to
501 allow full hydration of the GCL to take place. There is a need to provide a time lag between
502 completion of the construction of the pond and start of the filling process with saline water at
503 elevated temperatures. Failure to do so will result in potential desiccation of the GCL which could
504 be detrimental to the longevity of the pond.

505

506 **5. UNSATURATED SOIL-GEOSYNTHETIC INTERFACE SHEAR STRENGTH**

507

508 Waste containment cover or basal liner systems are often composed of several layers of
509 geosynthetics and natural soils. They must not only provide a sound hydraulic/gas barrier but must
510 also be structurally stable during all phases of a project (i.e., during construction, operation, and
511 closure). The interfaces between the different material layers composing a multi-layered lining
512 system often represent potential slip surfaces that need to be considered in slope stability analyses.
513 The shear strength of these interfaces are assessed by conducting shear tests on the interfaces using
514 direct shear box tests. In most cases these parameters are measured under water-saturated (wet) or
515 air-saturated (dry) conditions. Therefore, they are expressed in terms of total normal stresses rather
516 than effective normal stresses at the interface. Typically, the soil component of a multi layered liner
517 is unsaturated under normal working conditions (i.e., clay liner is installed at optimum moisture
518 content at degree of saturation ranging between 80 to 90%). Therefore, the initial suction and its
519 change during shearing might have an influence on the final value of the interface shear strength.

520

521 It is well known in unsaturated soil mechanics that matric suction plays an important role in the
522 inter-particle or effective stress state in unsaturated soils (Bishop 1959, Blight, 1967, Fredlund and
523 Morgenstern 1977, Khalili et al. 2004, Lu and Likos 2006, Nuth and Laloui 2008, Lu et al. 2010).
524 An increase in effective stress in unsaturated soils can lead to significant improvements in
525 engineering properties including shear strength and stiffness of soils (Lu and Likos 2006) and soil-
526 geosynthetic interaction (Hamid and Miller 2009).

527

528 The definition of effective stress in unsaturated soils has been a topic of some debate over the past
529 50 years. While the use of two independent stress-state variables proposed by Fredlund and
530 Morgenstern (1970) has led to some success in fitting constitutive models to experimental data, this
531 approach has received criticism because it cannot be reconciled with classical saturated soil

532 mechanics (Khalili et al. 2004, Nuth and Laloui 2008) and may require addition parameters to
533 represent changes in strength (Gan et al. 1988, Vanapalli et al. 1996). Bishop (1959) developed one
534 of the first equations to represent the effective stress σ' in unsaturated soils:

$$\sigma' = (\sigma - u_a) + \chi(u_a - u_w) \quad [2]$$

536
537 where σ is the total stress, u_a is the pore air pressure, u_w is the pore water pressure, and χ is the
538 effective stress parameter. The value of χ has been defined as the degree of saturation (Nuth and
539 Laloui 2008), as an empirical relationship incorporating the air entry suction (Khalili and Khabbaz
540 1998), and the effective saturation (Lu et al. 2010). Although the definition of effective stress by
541 Bishop (1959) initially received criticism because the role of matric suction in the effective stress
542 varies with the degree of saturation (Blight 1967) and in predicting collapse (Jennings and Burland
543 1963), several recent studies have proposed practical ways to define the single-value effective stress
544 variable (Khalili et al. 2004, Lu and Likos 2006, Nuth and Laloui 2008) and shown that it can be
545 used to represent shear strength (Khalili and Khabbaz 1998, Lu and Likos 2008) and predict
546 collapse (Khalili et al. 2004). A recent development in the equation for the effective stress was
547 made by Lu et al. (2010), who assumed that Bishop's χ factor was equal to the effective saturation,
548 which permits integration of the SWRC into Eq. 2.

$$\sigma' = \sigma - u_a + \frac{(u_a - u_w)}{(1 + [\alpha(u_a - u_w)]^n)^{(n-1)/n}} \quad [3]$$

550
551 where α and n are the van Genuchten SWRC parameters. Lu et al. (2010) found that Eq. 3 can be
552 used to interpret the shear strength of both unsaturated and saturated soils presented in the literature.

553

554 Very few studies have been conducted on unsaturated soil-geosynthetics interfaces. Only recently
555 that the effects of suction on soil-geosynthetic interface shear strength started to be investigated
556 (Sharma et al. 2007, Hatami et al. 2008, Hamid and Miller 2009, Khoury et al. 2010). These studies
557 have incorporated a two stress-state variable approach to interpret the effects of suction as shown in
558 Figures 16(a) and 16(c), but a reinterpretation of the data from a series of unsaturated direct shear
559 tests involving unsaturated clay and a nonwoven geotextilte indicates that Eq. 3 is suitable to
560 interpret their interface shear strength behaviour, as shown in Figure 16(d). The van Genuchten
561 (1980) SWRC parameters for the soil from Figure 16(b) were used to define the effective stress at
562 the interface using Eq. 3. The results in Figure 16 indicate that, similar to soils, greater effective
563 stress associated with higher suctions leads to an improvement in soil-geosynthetic interaction.

564

565 **6. GEOSYNTHETICS FOR SOIL REMEDIATION**

566

567 Many sites are faced with the problem of near surface soil contamination. Remediation of these
568 sites includes usually in situ treatment of the soil using different conventional remediation
569 techniques (e.g., bioremediation, vacuum/air stripping, soil flushing, encapsulation, excavation and
570 replacement of the contaminated soils with clean fill, etc.). However, we have seen in the past few
571 years the emergence of geosynthetics as part of the remediation process. Collazos et al., (2002,
572 2003) investigated the possibility of incorporating prefabricated vertical drains, composite
573 geosynthetic systems consisting of an inner core and a nonwoven geotextile outer filter jacket and
574 typically measuring 100 mm in width and about 6 mm in thickness, into soil vapour extraction
575 (SVE) systems to enhance their effectiveness. Soil vapour extraction (SVE) uses an induced flow
576 of air through the unsaturated zone to remove gases and vapours. In the most commonly practiced
577 method of application, a vacuum source (e.g., a blower or vacuum pump) is connected to a well,
578 which is screened across the contaminated interval of the unsaturated zone. The reduced pressure
579 within the well bore induces air flow toward the well from the surrounding soils. As the air flows

580 through the contaminated soils, the portion of volatile compounds present in the vapour phase, or
581 gas flows toward the well and is removed through the well along with the extracted air.
582 Prefabricated vertical drains were used to place “wells” at close spacing’s thus decreasing the travel
583 time for air to pass through the soil and increasing the opportunity for interception of the
584 contaminant. The many vents or extraction points afforded by the drains provide more options for
585 better control of the flow regime (Figure 17).

586

587 Collazos et al., (2002, 2003) work showed that PVD enhanced soil vapour extraction systems were
588 able to capture methane gas migrating laterally from a landfill. This was made possible by
589 shortening the air flow path to expedite contaminant removal time. To maximise further the
590 efficiency of the PVD enhanced systems Abuel-Naga and Bouazza, (2008) recommended the
591 modification of the structure of PVD (cross-section area, core shape) to allow it to handle higher
592 air/gas flow rates with minimum internal well resistance. Enhancing PVD flow efficiency will
593 increase its flow rate and the radius of pressure influence under similar pressure-controlled
594 extracting conditions.

595

596 **7. CONCLUSIONS**

597

598 This paper provides an insight into the interaction between soils and geosynthetics under
599 unsaturated conditions and highlights the significance of the unsaturated properties of
600 geosynthetics. The salient conclusions that can be drawn from this paper are:

601

- 602 • The water retention curve of geotextiles shows a highly nonlinear response, with a significant
603 decrease in water content (or degree of saturation) within a comparatively narrow range of
604 suction similar to coarse grained materials.

- 605 • The water retention curve of geosynthetic clay liners seems to be dependent on the
606 manufacturing process. However at higher suctions, the bentonite component tends to govern
607 the retention behaviour.
- 608 • The hydraulic conductivity of unsaturated geomaterials with relatively large pores such as
609 geotextiles (e.g. gravel, geotextiles) decreases faster than that of fine-grained soils. This
610 phenomenon leads to the counterintuitive situation in which the hydraulic conductivity of
611 unsaturated geotextiles can be significantly smaller than that of fine-grained soils.
- 612 • Recent column studies have clearly shown the development of a capillary break at the interface
613 between soils and an underlying nonwoven geotextile. Information from the water retention
614 curve and hydraulic function of the components of a capillary barrier can be used to predict the
615 breakthrough suction and water storage expected in the fine-grained component.
- 616 • Their capillary break potential behaviour has potential implications on the design of landfill leak
617 detection systems and performance evaluation of alternative cover systems for waste
618 containment facilities.
- 619 • The development of geosynthetic capillary barriers may benefit a number of geoenvironmental
620 engineering applications. However, poor performance of earth structures involving nonwoven
621 geotextiles may result from ignoring the capillary break effect.
- 622 • The hydration of geosynthetic clay liners depends on the water retention curve of the geosynthetic
623 clay liner.
- 624 • The hydraulic performance geosynthetic clay liners in an engineered liner system subjected to
625 elevated temperatures depends on the water retention curve of the geosynthetic clay liner. This
626 needs to be taken into account in the planning and operation of containment facilities involving heat
627 generated from waste.
- 628 • Greater effective stress associated with higher suctions leads to an improvement in soil-
629 geosynthetic interaction
- 630 • Geosynthetics can assist in accelerating soil remediation processes in unsaturated soils.

631 **REFERENCES**

632

633 ASTM (1995). ASTM Standards on Geosynthetics. Sponsored by ASTM Committee D-35 on Geosynthetics, Fourth
634 Edition, 178 p.

635

636 Abuel-Naga, H. and Bouazza, A. (2010). A novel laboratory techniques to determine the water retention curve of
637 geosynthetic clay liners. *Geosynthetics International*, Vol. 17, No5, pp. 313-322.

638

639 Abuel-Naga, H., Bouazza, A. Bowders, J. and Collazos, O. (2008). Numerical evaluation of prefabricated vertical drain
640 enhanced soil vapour extraction system. *Geosynthetics International* , Vol. 15, No3,pp.216-223.

641

642 Aydilek, A. H., D'Hondt, D. and Holtz, R. D. (2007). Comparative Evaluation of Geotextile Pore Sizes Using Bubble
643 Point Test and Image Analysis. *Geotechnical Testing Journal*, 30(3), 173–181.

644

645 Barroso, M., Touze-Foltz, N. and Saidi, F.K. (2006). Validation of the use of filter paper suction measurements for the
646 determination of GCL water retention curves. *Proceedings of the Eighth International Conference on Geosynthetics*,
647 Yokohama: 171–174.

648

649 Beddoe, R. A., Take, W. A. and Rowe, R. K. (2010). Development of suction measurement techniques to quantify the
650 water retention behaviour of GCLs. *Geosynthetics International*, 17, No. 5, 301-312.

651

652 Beddoe, R. A., Take, W. A. and Rowe, R. K. (2011). Water retention of geosynthetic clay liners. *Journal of*
653 *Geotechnical and Geoenvironmental Engineering*. doi:10.1061/(ASCE)GT.1943-5606.0000526

654

655 Benson, C. and Gribb, M. (1997). Measuring unsaturated hydraulic conductivity in the laboratory and field. *Unsaturated*
656 *Soil Engineering Practice*. Houston, S. and Wray, W. (eds). ASCE. Reston, VA. p. 113-168.

657

658 Bishop, A.W. (1959). The principle of effective stress. *Teknisk Ukeblad I Samarbeide Med Teknikk*, Oslo, Norway.
659 106(39), 859-863.

660

661 Blight, G. E. (1967). Effective stress evaluation for unsaturated soils. *J. Soil Mech. Found. Div. Am. Soc. Civ. Eng.* 93,
662 125-148.

663

664 Brooks, R.H. and Corey, A.T. (1964). Hydraulic properties of porous medium. Colorado State University (Fort
665 Collins). Hydrology Paper No. 3. March.

666

667 Bouazza, A., (2010). Geosynthetics in mining applications. Proceeding 6th International Congress on Environmental
668 Geotechnics, New Delhi, India, Vol.1, pp.221-259.

669

670 Bouazza, A. (2002). Geosynthetic clay liners. *Geotextiles and Geomembranes*, Vol. 20. No1, pp.3-17.

671

672 Bouazza, A. and Bowders, J.Jr. (2010). Geosynthetic clay liners for waste containment facilities, CRC Press, Taylor and
673 Francis Group, 254p.

674

675 Bouazza, A., Nahlawi, H. and Aylward, M. (2011). In-situ temperature monitoring in an organic waste landfill cell.
676 *Journal of Geotechnical and Geoenvironmental Engineering* [doi:10.1061/(ASCE)GT.1943-5606.0000533]

677

678 Bouazza, A., Zornberg, J. and Adam, D. (2002). Geosynthetics in waste containments: recent advances. Proceedings 7th
679 International Conference on Geosynthetics, Nice, France, vol. 2, pp. 445-507.

680

681 Bouazza, A. Freund, M. and Nahlawi, H. (2006a). Water retention of nonwoven polyester geotextiles. *Polymer Testing*.
682 25(8), 1038-1043.

683

684 Bouazza, A., Zornberg, J.G., McCartney, J.S., and Nahlawi, H. (2006b). Significance of unsaturated behaviour of
685 geotextiles in earthen structures. *Australian Geomechanics Journal*, September, Vol. 41, No. 3, pp. 133-142.

686

687 Burdine, N.T. (1953). Relative permeability calculations from pore-size distribution data. *Petroleum Transactions of*
688 *the American Institute of Mining and Metallurgical Engineering*. 198, 71-77.

689

690 Collazos O.M., Bowders J.J. and Bouazza, A. (2002). Prefabricated vertical drains for use in soil vapour extraction
691 applications. *Transportation Research Record* **1786**, pp. 104-111

692

693 Collazos O. M., Bowders, J. J. and Bouazza, A. (2003). Laboratory evaluation of prefabricated vertical drains for use in
694 soil vapour extraction systems. *Ground Improvement* 7, No. 3, 103–110.
695

696 Daniel, D.E., Shan, H.-Y. and Anderson, J.D., (1993). Effects of partial wetting on the performance of the bentonite
697 component of a geosynthetic clay liner. *Geosynthetics '93, IFAI, St. Paul, MN, 3*: 1482–1496.
698

699 Fredlund, D.G., and Morgenstern, N.R. (1977). Stress state variables for unsaturated soils. *ABB Rev.*, 103(5), 447–466.
700

701 Fredlund, D.G. and Xing, A. (1994). Equations for the soil-water characteristic curve. *Canadian Geotechnical Journal*.
702 31, 521-532.
703

704 Gan, J. K. M., D. G. Fredlund, and H. Rahardjo (1988). Determination of the shear strength parameters of an
705 unsaturated soil using the direct shear test. *Can. Geotech. J.*, 25, 500–510.
706

707 Gates, W.P., Bouazza, A. and Churchmann, J. (2009). Bentonite clay keeping pollutants at bay. *Elements*, Vol.5, No2,
708 pp. 105-110.
709

710 Hamid, T.B. and Miller, G.A. (2009). Shear strength of unsaturated soil interfaces. *Canadian Geotechnical Journal*. 46,
711 595-606.
712

713 Hillel, D. (1998). *Environmental Soil Physics*. ISBN 0-12-348525-8, Academic Press.
714

715 Hatami, K., Khoury, C.N., and Miller G.A. (2008). Suction-controlled testing of soil-geotextile interfaces.
716 *GeoAmericas*. Cancun, Mexico.
717

718 Hornsey, W.P., Scheirs, J., Gates, W.P. and Bouazza, A. (2010). The impact of mining solutions/liquors on
719 geosynthetics. *Geotextiles and Geomembrane*, Vol. 28, No2, pp.191-198.
720

721 Iryo, T. and Rowe, R.K. (2005). Hydraulic behaviour of soil-geocomposite layers in slopes. *Geosynthetics*
722 *International*. 12(3), 145-155.
723

724 Jennings, J.E.B. and Burland, J.B. (1962). Limitations to the use of effective stress in partly saturated soils.
725 Geotechnique. 12(2), 125-144.
726

727 Koerner, R. (2005). Designing With Geosynthetics. 5th Edition. Prentice Hall, NJ.
728

729 Koerner, G.R. and Koerner, R.M. (2006). Long term temperature monitoring of geomembranes at dry and wet landfills.
730 Geotextiles and Geomembranes, **24** (1):72-77.
731

732 Khalili, N., and Khabbaz, M. H. (1998). A unique relationship for χ for the determination of the shear strength of
733 unsaturated soils. Geotechnique,48(5), 1-7.
734

735 Khalili, N., Geiser, F., and Blight, G.E. (2004). Effective stress in unsaturated soils, A review with new evidence. Int. J.
736 Geomech., 4(2), 115-126.
737

738 Khoury, C.N., Miller, G.A., and Hatami, K. (2010). Shear strength of unsaturated soil-geotextile interfaces.”GeoFlorida
739 2010. Advances in Analysis, Modeling and Design. GSP 199. pp. 307-316.
740

741 Kool, J. B. and Parker, J. C. (1987). Development and evaluation of closed-form expression for hysteretic soil hydraulic
742 properties. Water Resources Research, 23, 105-114.
743

744 Lefebvre, X., Lanini, S. and Houi, D. 2000. The role of aerobic activity on refuse temperature rise, I. landfill
745 experimental study. Journal of Waste Management and Research, **18**:444-452
746

747 Lu, N. and Likos, W.J. (2006). Suction stress characteristic curve for unsaturated soil.”Journal and Geotechnical and
748 Geoenvironmental Engineering. 132(2), 131-142.
749

750 Lu, N., Godt, J.W. and Wu, D.T. (2010). A closed-form equation for effective stress in unsaturated soil. Water
751 Resources Research. 46, 14 pg.
752

753 Lourenco, S. D. N., Gallipoli, D., Toll, D., Evans, F. and Medero, G., (2007). Discussion: The development of a suction
754 control system for a triaxial apparatus. Geotechnical Testing Journal, 30, No. 4: 1-3.
755

756 McCartney, J.S., Kuhn, J.A. and Zornberg, J.G. (2005). Geosynthetic Drainage Layers in Contact with Unsaturated
757 Soils. Proceedings 16th International Conference of Soil Mechanics and Geotechnical Engineering, Osaka, Japan,
758 September 12-17, pp. 2301-2305.

759

760 Nahlawi, H., Bouazza, A. and Kodikara, J.K. (2007). Characterisation of geotextiles water retention using a modified
761 capillary pressure cell. *Geotextiles and Geomembranes*, Vol. 25, No. 3, pp. 186–193.

762

763 Nahlawi, N. (2009). Numerical and experimental investigation of the unsaturated hydraulic behaviour of geotextiles.
764 PhD Thesis, Department of Civil Engineering, Monash University, Australia.

765

766 Nuth, M., and L. Laloui (2008). Effective stress concept in unsaturated soils: Clarification and validation of a unified
767 framework. *Int. J. Numer. Anal. Methods Geomech.* 32, 771–801.

768

769 Palmeira, E. and Gardoni, M. (2002). Drainage and filtration properties of non-woven geotextiles under confinement
770 using different experimental techniques. *Geotextiles and Geomembranes*. 20, 97-115.

771

772 Rowe, R.K. (2005). Long term performance of contaminant barrier systems. *Geotechnique*, **55** (9):631-678.

773

774 Rowe, R.K. and Hoor, A. (2009). Predicted temperatures and service lives of secondary geomembrane landfill liners.
775 *Geosynthetics International* 16 (2):71-82.

776

777 Sharma, J.S., Fleming, I.R., and Jogi, M.B. (2007). Measurement of unsaturated soil-geomembrane interface shear
778 strength parameters. *Canadian Geotechnical Journal*. 44, 78-88.

779

780 Singh, R.M. (2007). An experimental and numerical investigation of heat and mass movement in unsaturated clays.
781 Ph.D. thesis, Cardiff School of Engineering, Cardiff University, UK.

782

783 Southen, J. M. and Rowe, R.K. (2007). Evaluation of the water retention curve for geosynthetic clay liners. *Geotextiles*
784 *and Geomembranes*, 25(1) : 2-9.

785

786 Thomas HR and He Y (1994). A coupled heat-moisture transfer theory for deformable unsaturated soil and its
787 algorithmic implementation. *International Journal for Numerical Methods in Engineering*, 40: 3421-3441.

788 Topp, G.C. and Miller, E.E. (1966). Hysteretic water characteristics and hydraulic conductivities for glass-bead media.
789 Soil Sci. Soc. Am. Proc. 30:156-162.
790

791 Vanapalli, S. K., D. E. Fredlund, D. E. Pufahl, and A. W. Clifton (1996). Model for the prediction of shear strength with
792 respect to soil suction. Can. Geotech. J., 33, 379–392.
793

794 van Genuchten, M. (1980). A closed-form equation for predicting the hydraulic conductivity of unsaturated soils. Soil
795 Sci. Soc. Am. Proc. 44, 892-898.
796

797 Wang, X. and Benson, C.H. (2004). Leak-free pressure plate extractor for the soil water characteristic curve.
798 Geotechnical Testing Journal. 27(2), 1-10.
799

800 Williams, L.O., Hoyt, D.L., Hargreaves, G.A., Dwyer, S.F. and Zornberg, J.G. (2010). Evaluation of a capillary barrier at
801 the Rocky Mountain Arsenal. Proceedings 5th International Conference on Unsaturated Soils, Barcelona, Spain, Vol.2,
802 pp. 1431-1436.
803

804 Williams, L.O., Dwyer, S.F., Zornberg, J.G., Hoyt, D.L. and Hargreaves, G.A. (2011). Covering it all. Journal of Civil
805 Engineering, ASCE, January, pp.65-71.
806

807 Yesiller, N., Hanson, J.L. and Liu, W.L. (2005). Heat generation in municipal solid waste landfills. Journal of
808 Geotechnical and Geoenvironmental Engineering, **131** (11):1330-1344.
809

810 Yoshida, H., Hozumi, H. and Tanaka, N. (1996). Theoretical Study on Temperature Distribution in a Sanitary Landfill,
811 Proceedings 2nd International Congress on Environmental Geotechnics, Osaka, Japan, **1**:323-328.
812

813 Zornberg, J.G. and Christopher, B.R. (2007). Chapter 37: Geosynthetics. In: The Handbook of Groundwater
814 Engineering, 2nd Edition, Jacques W. Delleur (Editor-in-Chief), CRC Press, Taylor and Francis Group, Boca Raton,
815 Florida.
816

817 Zornberg, J.G., Bouazza, A. and McCartney, J.S. (2010). Geosynthetic capillary barriers: current state of knowledge.
818 Geosynthetics International, Vol.17, 5, pp.273-300.

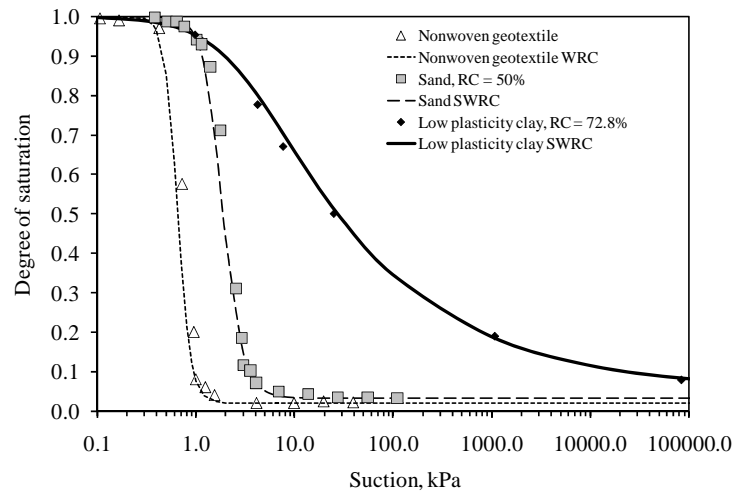


Figure 1. Typical WRCs for different geotechnical materials (after McCartney *et al.* 2005)

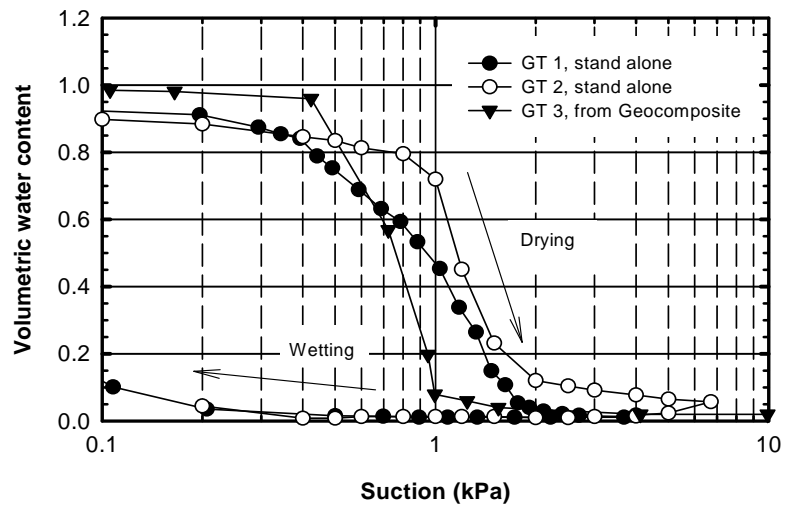


Figure 2. Geotextile water retention curves.

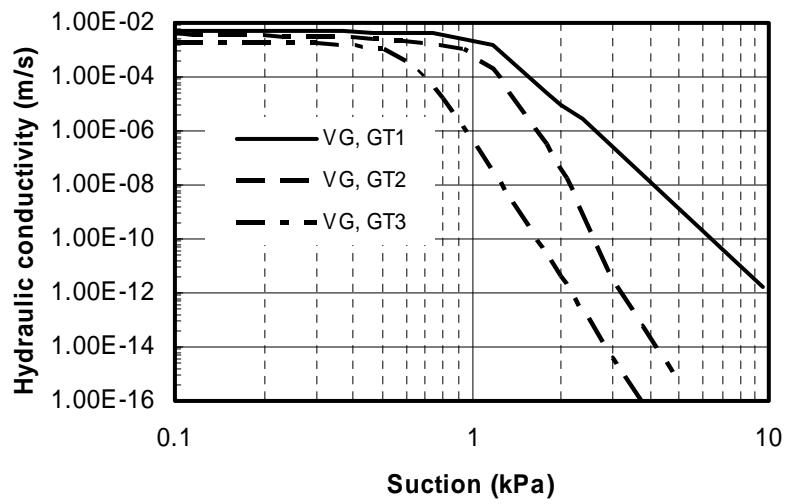


Figure 3. Hydraulic conductivity functions of different geotextiles.

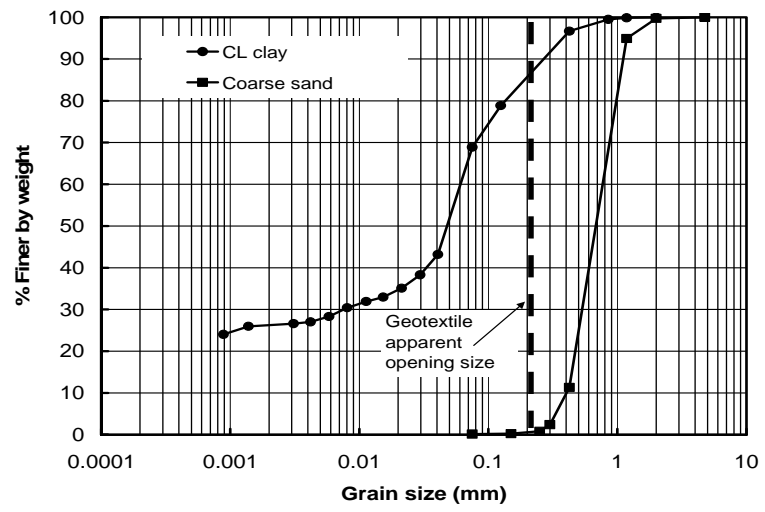


Figure 4. Comparison between the clay and sand grain size distributions with the apparent opening size of a nonwoven geotextile

Figure

[Click here to download Figure: Figure 5.pdf](#)

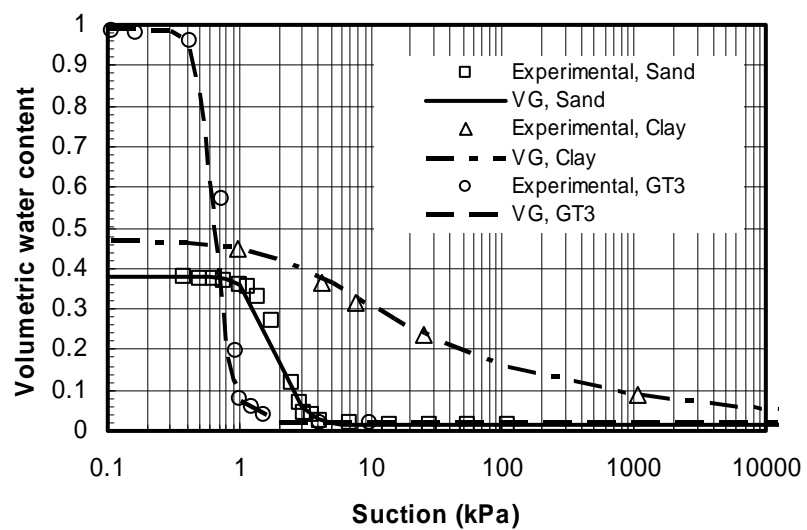


Figure 5. Water retention curves for soils and geocomposites (note: VG=van Genuchten equation)

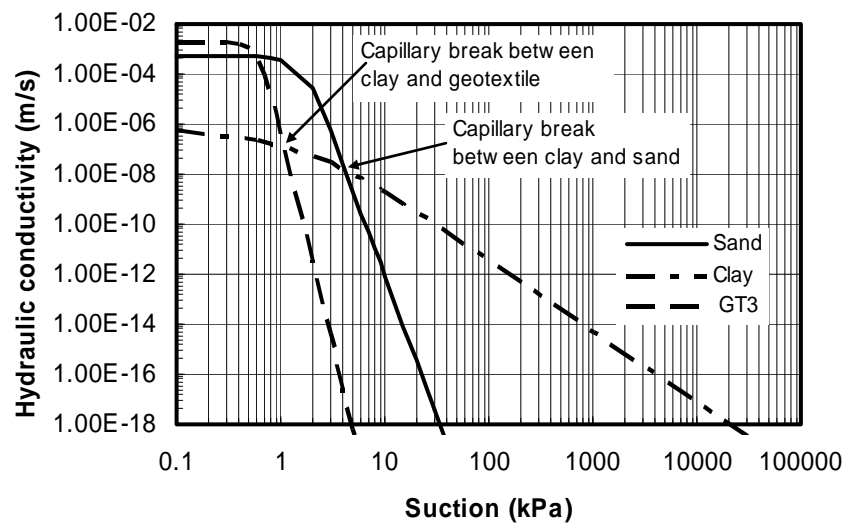


Figure 6. Predicted hydraulic conductivity functions (k -functions) of soils and geocomposites

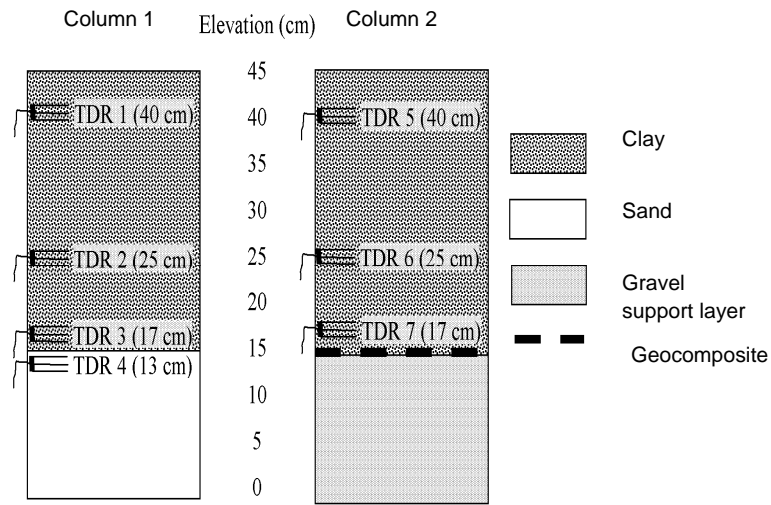


Figure 7. Schematic view of infiltration columns

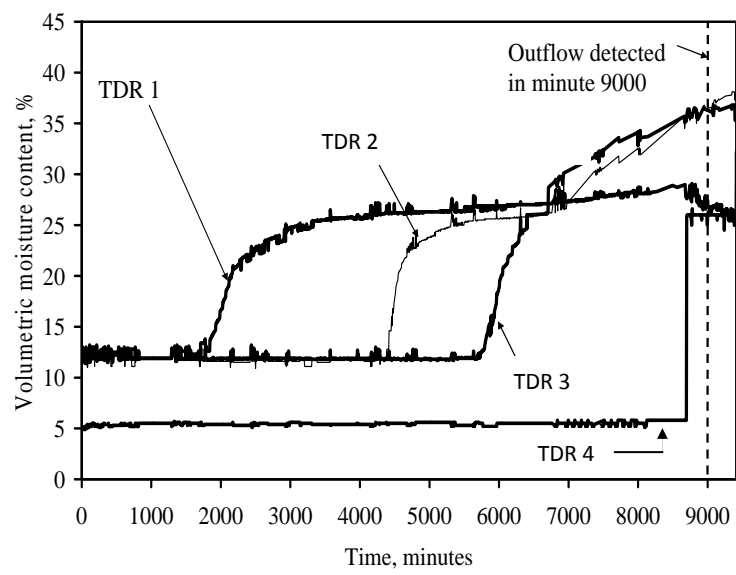


Figure 8. Volumetric moisture content with depth in Column 1

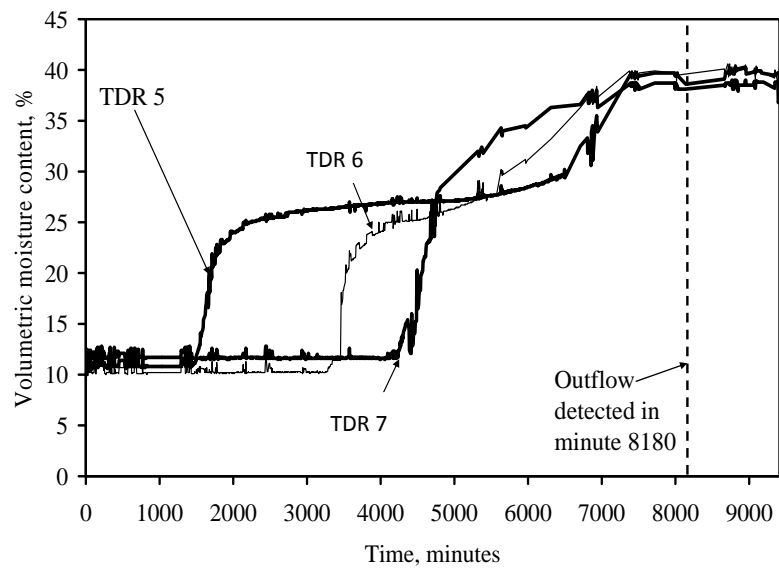


Figure 9. Volumetric moisture content with depth in Column 2

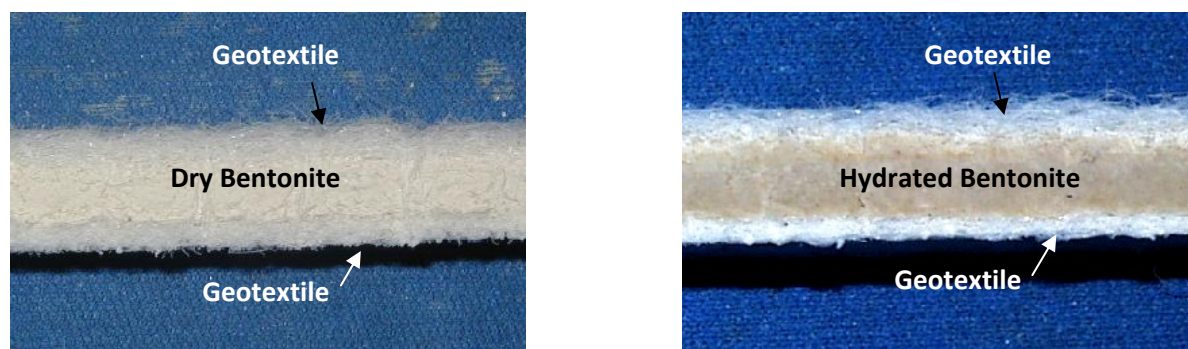


Figure 10. Geosynthetic clay liner under dry and fully hydrated conditions

Figure

[Click here to download Figure: Figure 11.pdf](#)

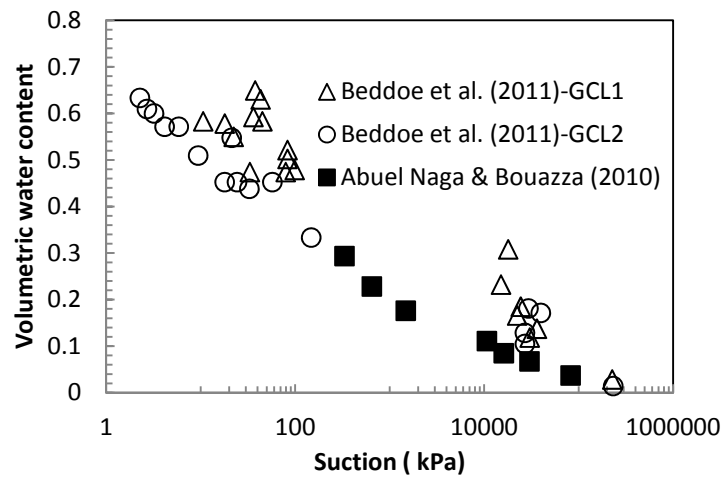


Figure 11. Water retention of GCLs under wetting path.

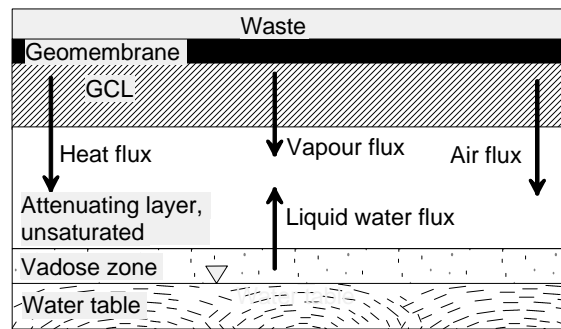


Figure 12. Thermally induced multiphase fluid transport processes within and beneath a composite liner

Figure

[Click here to download Figure: Figure 13.pdf](#)

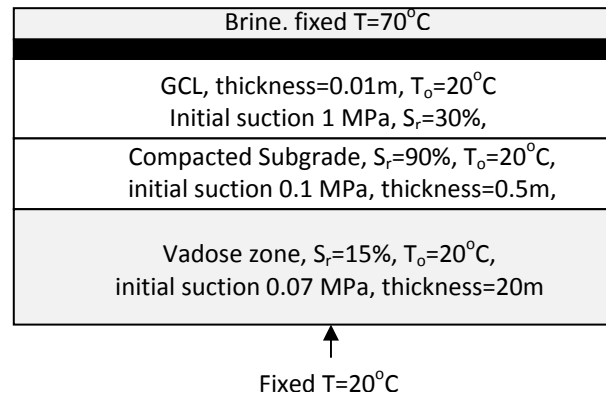


Figure 13. Cross section of composite liner and soil profile for an evaporative pond.

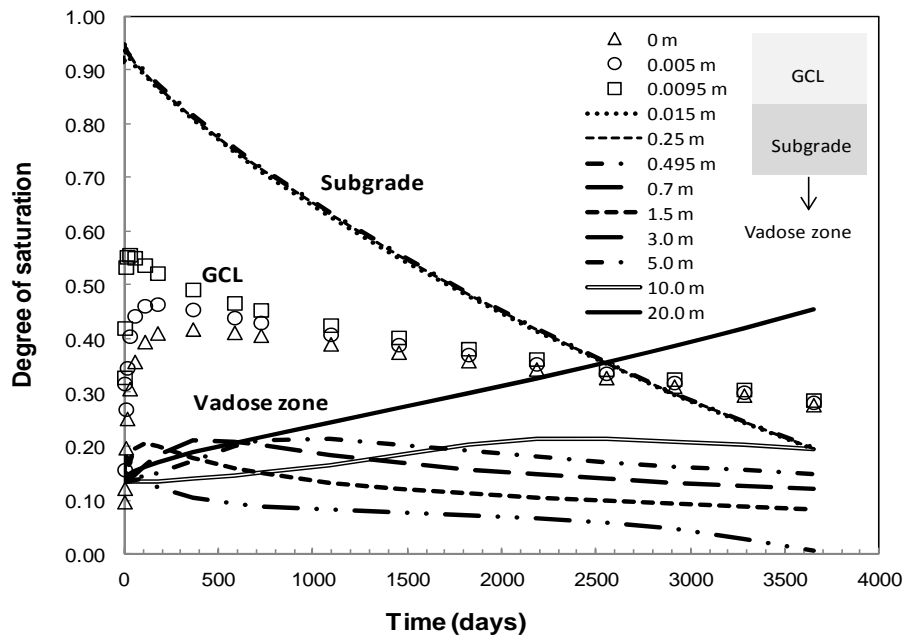


Figure 14. Degree of saturation variation with time for a GCL, subgrade, and underlying soils

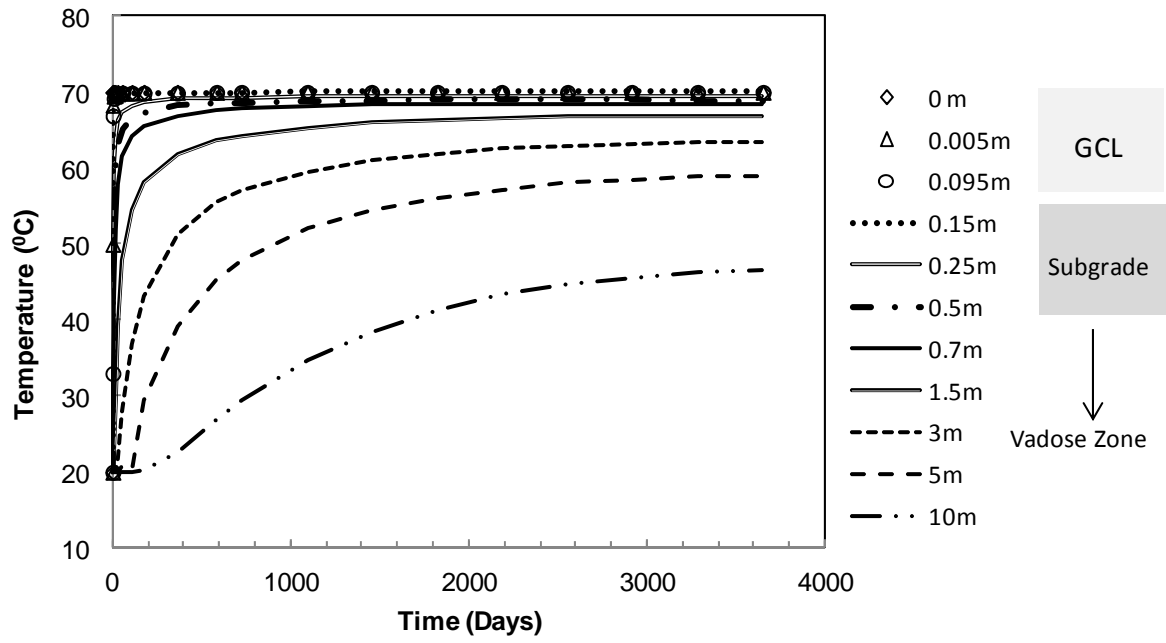


Figure 15. Temperature variation with time

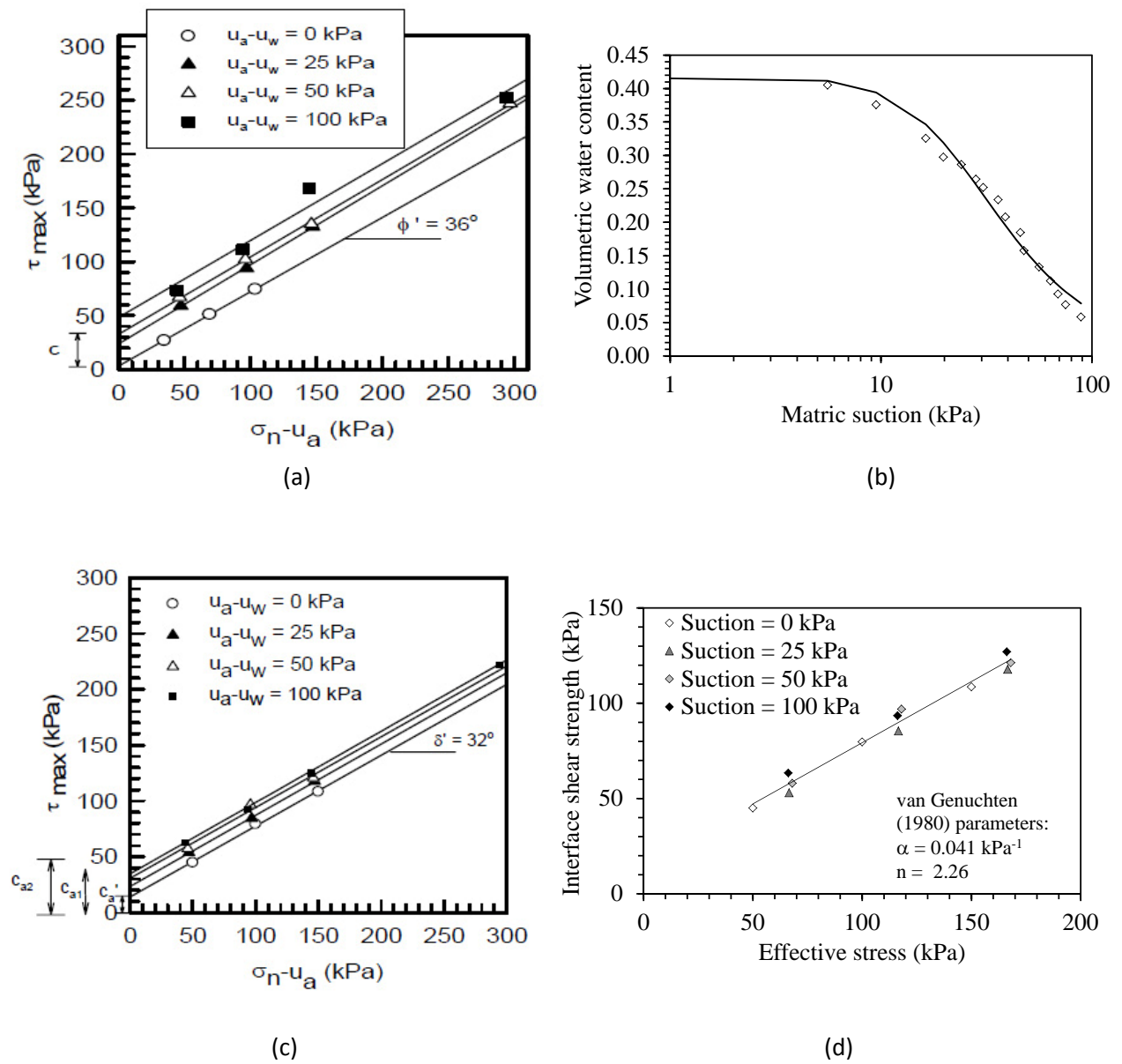


Figure 16. Unsaturated interface shear strength from Khoury et al. (2010): (a) Shear strength of unsaturated soil; (b) SWRC for the soil; (c) Shear strength of soil-geosynthetic interface; (d) Shear strength of soil-geosynthetic interface reinterpreted using Eq. 3

Figure

[Click here to download Figure: Figure 17.pdf](#)

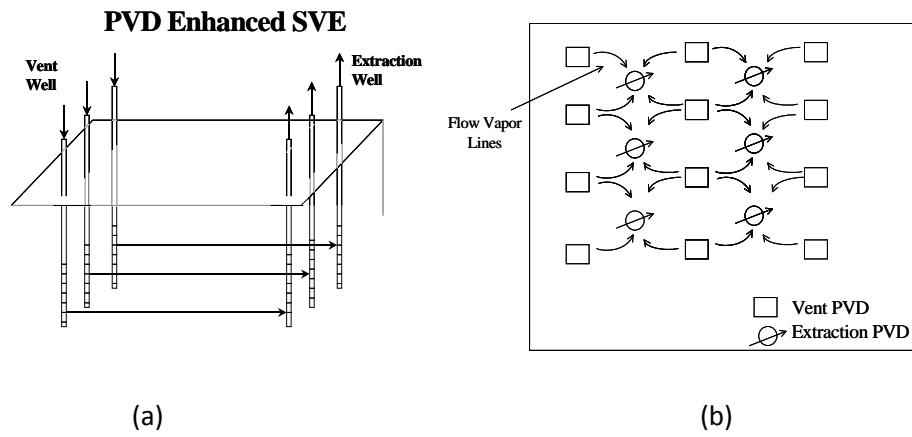


Figure 17. (a) Vent and extraction PVDs (b) Flow path direction